

Garnet peridotites from Pohorje: Petrography, geothermobarometry and metamorphic evolution

Petrografija, geotermobarometrija in metamorfni razvoj granatovega peridotita na Pohorju

Mirijam VRABEC

University of Ljubljana, Faculty of Natural Sciences and Engineering, Department of Geology, Aškerčeva 12, SI-1000 Ljubljana, Slovenia; e-mail: mirijam.vrabec@ntf.uni-lj.si

Prejeto / Received 15. 3. 2010; Sprejeto / Accepted 20. 5. 2010

Key words: ultrahigh-pressure metamorphism, garnet peridotite, geothermobarometry, collisional orogen, Pohorje, Eastern Alps, Slovenia

Ključne besede: ultravisokotlačna metamorfoza, granatov peridotit, geotermobarometrija, kolizijski orogeni, Pohorje, Vzhodne Alpe, Slovenija

Abstract

Ultrahigh-pressure (UHP) metamorphism has been recorded in Eo-Alpine garnet peridotites from the Pohorje Mts., Slovenia, belonging to the Eastern Alps. The garnet peridotite bodies are found within serpentized meta-ultrabasites in the SE edge of Pohorje and are closely associated with UHP kyanite eclogites. These rocks belong to the Lower Central Austroalpine basement unit of the Eastern Alps, exposed in the proximity of the Periadriatic fault system.

Garnet peridotites show signs of a complex four-stage metamorphic history. The protolith stage is represented by a low-P high-T assemblage of olivine + Al-rich orthopyroxene + Al-rich clinopyroxene + Cr-spinel. Due to metamorphism, primary clinopyroxene shows exsolutions of garnet, orthopyroxene, amphibole, Cr-spinel and ilmenite. The UHP metamorphic stage is defined by the assemblage garnet + olivine + Al-poor orthopyroxene + clinopyroxene + Cr-spinel. Subsequent decompression and final retrogression stage resulted in formation of kelyphitic rims around garnet and crystallization of tremolite, chlorite, serpentine and talc.

Pressure and temperature estimates indicate that garnet peridotites reached the peak of metamorphism at 4 GPa and 900 °C, that is well within the UHP stability field. Garnet peridotites in the Pohorje Mountains experienced UHP metamorphism during the Cretaceous orogeny and thus record the highest-pressure conditions of all Eo-Alpine metamorphism in the Alps.

Izvleček

Granatovi peridotiti na JV robu Pohorja kažejo znake metamorfoze pri ultravisokotlačnih pogojih. Nastopajo v obliki majhnih teles znotraj serpentiniziranih metaultrabazičnih kamnin in so v tesni povezavi z ultravisokotlačnimi kyanitovimi eklogiti. Tako peridotiti kot eklogiti pripadajo kamninam Spodnjega srednjega avstroalpina Vzhodnih Alp.

Metamorfni razvoj granatovih peridotitov je potekal v štirih fazah. Protolitna faza obsega nizkotlačno in visokotemperaturno mineralno združbo olivin + visoko-Al ortopiroksen + visoko-Al klinopiroksen + Cr-spinel. Med metamorfozo so se v primarnih klinopiroksenih formirale eksolucijske lamele granata, ortopiroksena, amfibola, Cr-spinela in ilmenita. Fazo ultravisokotlačne metamorfoze označujejo minerali granat + olivin + nizko-Al ortopiroksen + klinopiroksen + Cr-spinel. Sledili sta dekomprisijska in kot zadnja retrogradna faza, ki je nastopila pri najnižjih P-T pogojih. To zaznamujejo nizkotemperaturni minerali, kot so tremolit, klorit, serpentin in lojvec.

Geotermobarometrični izračuni kažejo, da so bili granatovi peridotiti na Pohorju med viškom metamorfoze v času kredne orogeneze izpostavljeni tlaku 4 GPa in temperaturi preko 900 °C, kar ustreza polju ultravisokotlačne metamorfoze. Tako predstavljajo najvišje tlačne pogoje, dosežene med eo-alpinsko orogenezo na območju celotnega Alpskega orogena.

Introduction

Garnet peridotites are commonly associated with eclogites in UHP metamorphic terranes (LIU et al., 1998; CARSWELL & COMPAGNONI, 2003; CHOPIN, 2003). Peridotite massifs are important features of orogenic belts worldwide. Spinel peridotite is pre-

dominant in such bodies, but garnet peridotite is common in continental collision belts, particularly in Eurasian UHP metamorphic terranes (garnet peridotites and pyroxenites have been reported from 11 of the 15 or so HP/UHP terranes). These so-called 'orogenic' or 'Alpine-type' peridotites include several garnet-bearing rock types, such as

lherzolites, harzburgites, wehrlites, dunites and pyroxenites, generally referred to as garnet peridotites. These rocks mostly occur not only within metamorphosed continental crust, but also within units of oceanic affinity (e.g. BRUECKNER & MEDARIS, 2000 and references therein). Although volumetrically minor, these UHP metamorphic rocks provide an opportunity to evaluate the tectonothermal conditions related to the interaction of mantle and crust during UHP metamorphism as well as important information on orogenic processes in deep orogenic root zones and the upper mantle (e.g. ZHANG et al., 1994; DOBRZHINETSAYA et al., 1996; VAN ROERMUND & DRURY, 1998).

Most garnet peridotites are depleted upper mantle material, variously modified by metasomatism, but some originated by low-pressure crystallization from ultramafic-mafic igneous complexes. All presently known garnet peridotites in Eurasian HP/UHP terranes can be divided into two groups, one having a high P/T ratio and the other a low P/T ratio (MEDARIS, 2000; Figure 1). Nearly all of the peridotite occurrences in the high P/T group can be related to subduction processes and are isofacial and approximately contemporaneous with associated UHP crustal rocks that contain coesite and diamond. The single exception is the Western Gneiss Region, Norway, where the garnet peridotites are relicts of old, cold lithosphere that formed earlier and

under different conditions than those prevailing during the overprinting Caledonian metamorphism. Peridotites in the low P/T group are associated with HP crustal rocks that are characterized by HP granulites and strongly retrogressed eclogites, in which little evidence for the presence of coesite or diamond was found so far. The extremely high temperatures of the low P/T group would seem to require the influence of upwelling asthenosphere.

Garnet peridotites are thought to have evolved in at least four different tectonothermal settings (MEDARIS, 2000): (1) emplacement of peridotites (serpentinites or igneous complexes, e.g. ophiolite components or ultramafic differentiates of mafic intrusions) into the oceanic or continental crust prior to UHP metamorphism, followed by transport of peridotites and associated crust to UHP conditions (high P/T) by a subducting plate; (2) transfer of peridotites from a mantle wedge to the crust of an underlying, subducting plate (high P/T); such peridotites are initially either spinel- or garnet-bearing, depending on the depth of derivation; (3) originating from upwelling asthenosphere that passed through a high-temperature spinel peridotite stage, followed by cooling into the garnet peridotite field (low P/T); and (4) extraction of garnet peridotites from ancient subcontinental lithosphere, perhaps by deep-seated faulting within a continental plate (high P/T).

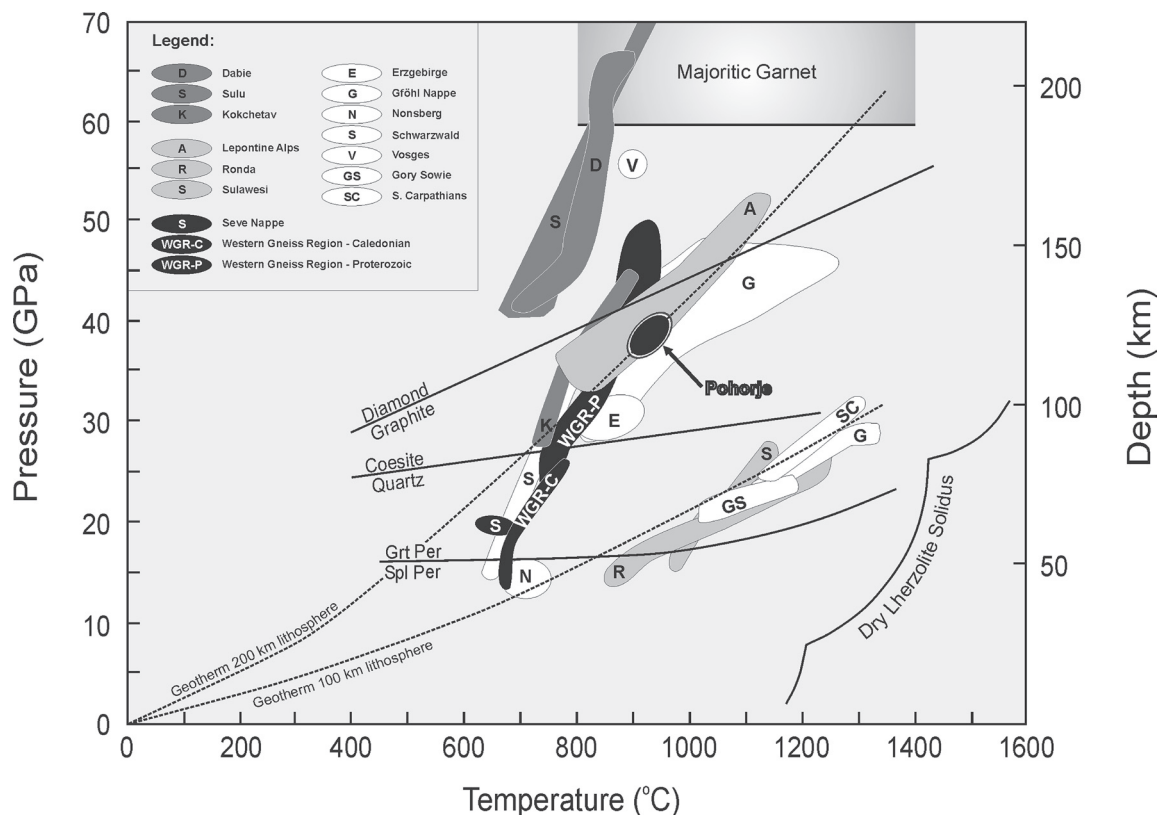


Figure 1. P-T estimates for Pohorje garnet peridotites in comparison with well established UHP terranes:

- (1) Asian UHP terranes (dark grey color);
- (2) Scandinavian Caledonides (black color);
- (3) European Variscan terranes (white color); and
- (4) Alpine terranes (pale grey color; after MEDARIS, 2000).

Shown for reference are equilibria for diamond-graphite (BUNDY, 1980), coesite-quartz (BOHLEN & BOETCHER, 1982), and spinel-garnet peridotite (O'HARA et al., 1971). Also shown are steady-state conductive geotherms for 200 km and 100 km thick lithosphere, a dry lherzolite solidus (TAKAHASHI, 1986), and a stability field for majoritic garnet containing 3 to 5 vol% pyroxene.

Garnet peridotite bodies in the Alps are known from two main regions. Alpe Arami, Monte Duria and Cima di Gagnone garnet peridotites belong to the Adula-Cima Lunga unit (ERNST, 1978; NIMIS & TROMMSDORFF, 2001; PAQUIN & ALTHERR, 2001), and are of Tertiary age (BECKER, 1993; GEBAUER, 1996), whereas garnet peridotites from Nonsberg area in the Ulten zone (OBATA & MORTEN, 1987; NIMIS & MORTEN, 2000) are of Variscan age (TUMIATI et al., 2003). Metamorphic processes related to the Cretaceous (so-called Eo-Alpine) events in the Alps have been recognized mainly in the Austroalpine units (e.g. THÖNI & JAGOUTZ, 1992; HOINKES et al., 1999; SCHMID et al., 2004; SCHUSTER et al., 2004). In the Eastern Alps, the metamorphic grade of Cretaceous metamorphism reached UHP facies in the south-easternmost parts, in the Pohorje Mountains of Slovenia, belonging to the Lower Central Austroalpine unit (JANÁK et al., 2004; VRABEC, 2010).

In kyanite eclogites from Pohorje Mountains UHP metamorphism have been recently documented (JANÁK et al., 2004; VRABEC, 2010). The eclogites are closely associated with serpentized metaultrabasites in which investigated garnet peridotite remnants are preserved (JANÁK et al., 2006). Early estimates of the P-T conditions experienced by the Pohorje garnet peridotites were in the range of 750–1050 °C and 2.4–3.6 GPa (HINTERLECHNER-RAVNIK et al., 1991; VISONA et al., 1991).

This paper presents the evidence for UHP metamorphism of garnet-bearing ultramafic rocks in the Austroalpine units of the Eastern Alps, exposed in the Pohorje Mountains of Slovenia. Described here are the mineralogical, petrological and geothermobarometrical features of garnet peridotites constraining their multi-stage metamorphic evolution. The obtained results offer additional evidence for UHP metamorphism in the Eastern Alps.

Geological Background

The Pohorje massif is built up of three Eo-Alpine Cretaceous nappes (MIOČ & ŽNIDARČIČ, 1977; FODOR et al., 2003) that belong to pre-Neogene metamorphic sequences of the Austroalpine units of the Eastern Alps (Figure 2). The lowest nappe that is termed the Pohorje nappe (JANÁK et al., 2006) represents the Lower Central Austroalpine (JANÁK et al., 2004) and consists of medium- to high-grade metamorphic rocks, predominantly micaschists, gneisses and amphibolites with marble and quartzite lenses. It also contains several eclogite lenses and a body of metaultrabasic rocks. The Pohorje nappe is overlain by a nappe composed of weakly metamorphosed Paleozoic rocks, mainly low-grade metamorphic slates and phyllites. The uppermost nappe is built up of Permo-Triassic clastic sedimentary rocks, mainly sandstones and conglomerates. The two latter nappes represent the Upper Central Austroalpine. The entire nappe stack is overlain by Early Miocene sediments which belong to the syn-rift basin fill of the Pannonian Basin (FODOR et al., 2003).

The magmatic intrusion in the central part of Pohorje is of Miocene age (18–19 Ma; TRAJANOVA et al., 2008; FODOR et al., 2007). It is of granodioritic to tonalitic composition (ZUPANČIČ, 1994), with a very small gabbroic enclave in its SE part. The main intrusion was followed by the formation of aplite and pegmatite veins, and lamprophyric dykes. In the western part of Pohorje, shallow dacite bodies and dykes intrude both the granodiorite body and the country rocks, suggesting that the dacite intrusion is somewhat younger than the granodiorite one. The Pohorje nappe is folded into an ESE-WNW-striking antiform, the core of which is occupied by the intrusion. Therefore, neither the original basal contact of the Pohorje nappe nor

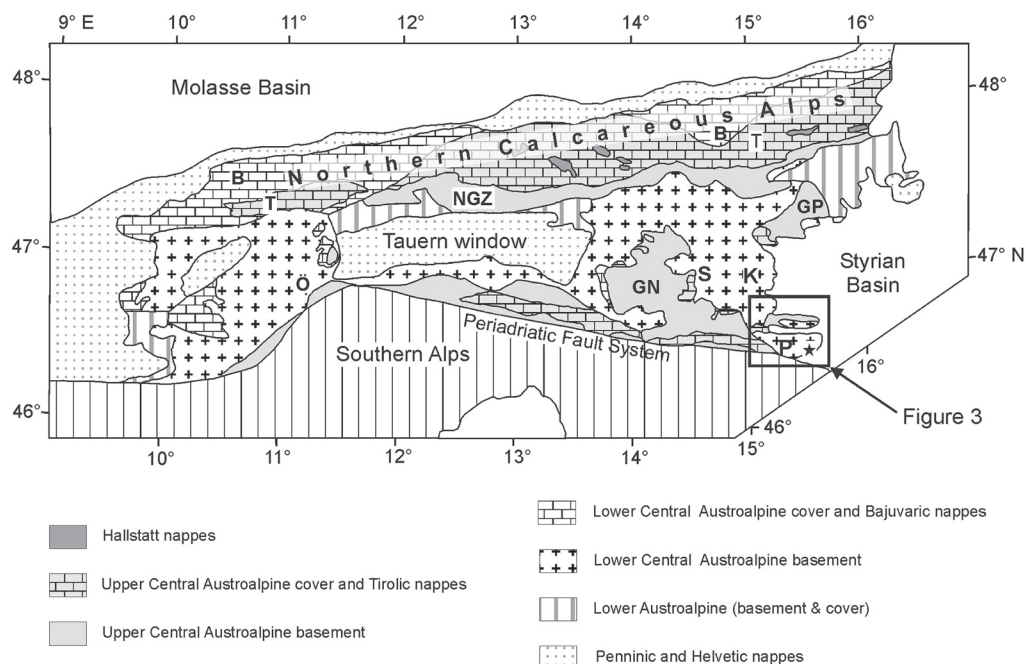


Figure 2. Tectonic map of the Eastern Alps. B-Bajuvaric, GN-Gurktal nappe, GP-Graz Paleozoic, K-Koralpe, NGZ-Northern Grauwacke zone, Ö-Southern Ötztal nappe, P-Pohorje, S-Saualpe, T-Tirolic. Modified after NEUBAUER & HÖCK (2000) and SCHMID et al. (2004).

any deeper tectonic units are exposed in the Pohorje area.

North and south of the granodiorite intrusion, eclogite bodies, lenses and bands of different sizes are found within country rocks. Numerous lenses, boudins and bands of eclogites also occur within the metaultrabasite body, located in the south-easternmost part of Pohorje Mountains near Slovenska Bistrica. Metaultrabasites form a body of ca. 5 x 1 km size, which is termed the Slovenska Bistrica ultramafic complex (SBUC; JANÁK et al., 2006; Figure 3). Some outcrops of garnet peridotites also occur away from this body, further to the west. The main protoliths of the Slovenska Bistrica ultramafic complex are harzburgites and dunites (cf. HINTERLECHNER-RAVNIK, 1987; HINTERLECHNER-RAVNIK et al., 1991). Because of extensive serpentinization, only a few less-altered bodies of garnet peridotites, garnet pyroxenites and coronitic metatroctolites are preserved (HINTERLECHNER-RAVNIK, 1987; HINTERLECHNER-RAVNIK et al., 1991). The country rocks of the eclogites and the Slovenska Bistrica ultramafic complex are amphibolites, orthogneisses, paragneisses and micaschists. These rocks form a strongly foliated matrix around elongated lenses and boudins of eclogites and ultrabasites, including the Slovenska Bistrica ultramafic complex.

The timing of HP/UHP metamorphism in the Pohorje nappe is Cretaceous, as documented by dating of eclogites with garnet Sm-Nd and zircon U-Pb ages of 91 Ma (MILLER et al., 2005). Almost identical ages have been obtained from dating of garnet (93–87 Ma; THÖNI, 2002) and zircon (92 Ma; JANÁK et al., 2009) of gneisses and micaschists. This age is similar to that of Korralpe and Saualpe eclogite facies metamorphism (THÖNI & JAGOUTZ, 1992; THÖNI & MILLER, 1996; MILLER & THÖNI, 1997; THÖNI, 2002). Tertiary K-Ar mica ages (19–13 Ma)

as well as apatite and zircon fission track ages (19–10 Ma) were obtained from the country rocks of eclogites and metaultrabasites in the Pohorje nappe (FODOR et al., 2002). This suggests that the peak of metamorphism was attained during the Cretaceous, and final cooling occurred in the Early to Middle Miocene. Upper Cretaceous (75–70 Ma) cooling ages were determined in the Korralpe area, the north-westward extension of the Pohorje nappe (SCHUSTER et al., 2004), indicating that the Korralpe rocks were exhumed during the Upper Cretaceous. Also the major exhumation of the Pohorje nappe, from UHP depth to crustal depth, most probably occurred already during the Upper Cretaceous. The final stage of exhumation to the surface was achieved in the Miocene by east- to north-east-directed low-angle extensional shearing, associated with the main opening phase of the Pannonian basin and leading to the core complex structure of the Pohorje Mountains (FODOR et al., 2003). The Miocene shearing event reactivated and overprinted the nappe boundaries in the Pohorje area (JANÁK et al., 2006). Therefore, direct structural evidence for the kinematics of Cretaceous exhumation has not yet been found.

Methods

Electron Probe Micro-Analysis

Microchemical analyses of the main constituent minerals were determined by Electron Probe Micro-Analysis (EPMA) technique using a CAMECA SX-100 electron microprobe at Dionýz Štúr Institute of Geology in Bratislava. Bombarding of micro-volumes of sample with a focused electron beam (5–30 keV) induced emission of X-ray photons. The wavelengths of collected X-rays

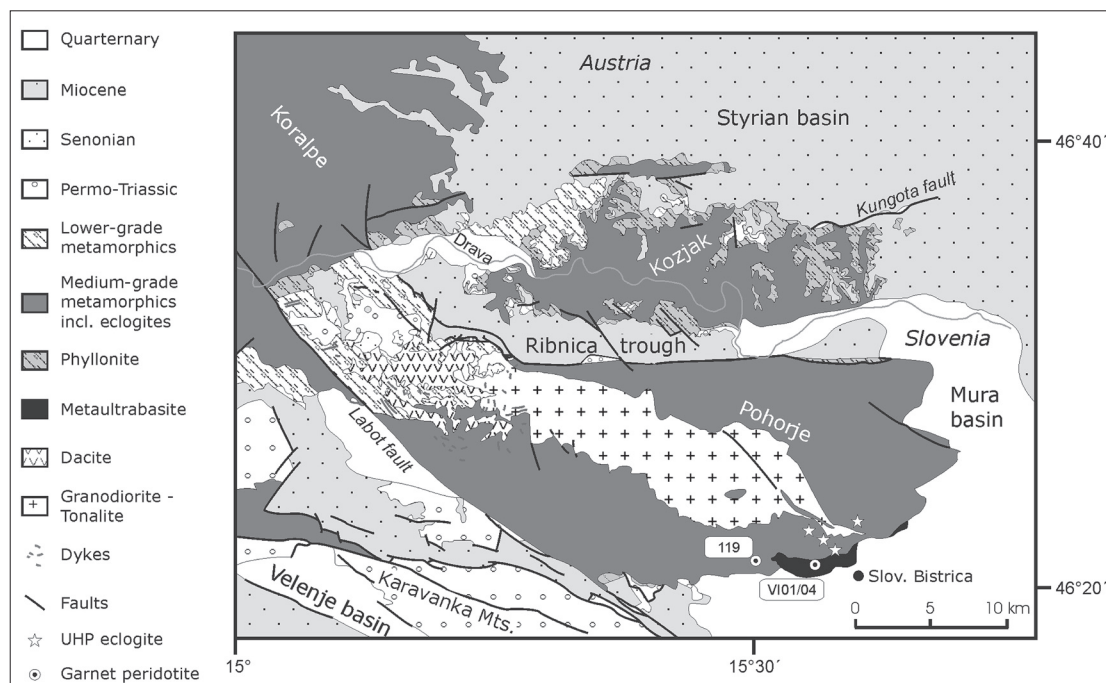


Figure 3. Simplified geological map of Pohorje and adjacent areas (modified from Mioč & Žnidarčič, 1977) showing locations of the investigated garnet peridotites. Locality VI01/04 is outcropping within the SBUC near Visole while the other one, locality 119, is exposed farther west, near Prihovca.

were identified by recording their WDS spectra (Wavelength Dispersive Spectroscopy). Analytical conditions were 15 keV accelerating voltage and 20 nA beam current, with a peak counting time of

20 s and a beam diameter of 2–10 μm . Raw counts were corrected using a PAP routine.

Representative analyses of mineral phases are given in Table 1.

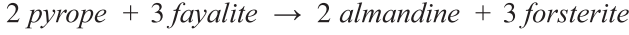
Table 1. Representative microprobe analyses of mineral compositions. I – protolith stage, II – metamorphic stage, III – decompression stage, IV – retrogression stage.

Sample	119	119	119	119	119	119	119	119	119	119	119
Mineral	Ol II	Grt II	Grt II ^{exs}	Cpx I, II	Opx II ^{exs}	Opx II	Opx III	Spl I, II	Spl III	Amp III	Amp IV
SiO ₂	40.70	41.40	41.95	54.02	58.26	57.73	56.50	0.01	0.04	45.23	56.16
TiO ₂	0.00	0.01	0.04	0.03	0.01	0.05	0.01	0.14	0.00	0.35	0.11
Al ₂ O ₃	0.03	23.20	22.70	0.93	0.85	0.74	1.97	27.78	69.64	12.49	2.26
Cr ₂ O ₃	0.01	0.12	1.05	0.16	0.17	0.11	0.03	35.43	0.00	0.77	0.30
FeO	10.69	10.02	12.13	1.78	6.93	6.55	6.32	25.50	7.79	5.18	3.73
MnO	0.10	0.24	0.46	0.02	0.10	0.10	0.08	0.29	0.00	0.02	0.08
MgO	49.90	18.80	16.56	17.52	34.81	35.64	34.70	10.30	23.20	18.41	21.89
CaO	0.02	5.46	5.81	24.90	0.56	0.20	0.21	0.00	0.06	12.14	12.93
Na ₂ O	0.00	0.00	0.00	0.42	0.00	0.00	0.01	0.00	0.00	2.70	0.30
K ₂ O	0.00	0.00	0.00	0.02	0.00	0.00	0.01	0.00	0.00	0.07	0.02
Total	101.44	99.25	100.70	99.80	101.69	101.12	99.84	99.45	100.73	97.36	97.79
Si	0.986	2.983	3.018	1.968	1.979	1.963	1.950	0.000	0.001	6.390	7.743
Ti	0.000	0.001	0.002	0.001	0.000	0.001	0.000	0.003	0.000	0.037	0.012
Al	0.001	1.971	1.925	0.040	0.034	0.030	0.080	1.004	1.994	2.080	0.367
Cr	0.000	0.007	0.060	0.005	0.005	0.003	0.001	0.858	0.000	0.086	0.032
Fe ²⁺	0.217	0.602	0.730	0.054	0.197	0.186	0.183	0.640	0.157	0.574	0.430
Mn	0.002	0.015	0.028	0.001	0.003	0.003	0.002	0.008	0.000	0.002	0.010
Mg	1.802	2.019	1.776	0.951	1.762	1.806	1.785	0.471	0.840	3.876	4.499
Ca	0.000	0.422	0.448	0.972	0.020	0.007	0.008	0.000	0.002	1.838	1.910
Na	0.000	0.000	0.000	0.030	0.000	0.000	0.000	0.000	0.000	0.740	0.082
K	0.000	0.000	0.000	0.001	0.000	0.000	0.000	0.000	0.000	0.013	0.004
Total	3.008	8.020	7.987	4.022	4.000	3.999	4.009	2.984	2.994	15.636	15.088
X _{Mg}	0.89	0.78	0.71	0.95	0.90	0.92	0.91	0.42	0.84	0.94	0.91
Cr*								0.46	0.00		
Sample	VI01/04	VI01/04	VI01/04	VI01/04	VI01/04	VI01/04	VI01/04	VI01/04	VI01/04	VI01/04	VI01/04
Mineral	Ol II	Grt II	Cpx I	Cpx II, III	Opx I	Opx II	Opx III	Spl I, II	Spl III	Amp III	Amp IV
SiO ₂	40.62	41.73	52.95	55.28	56.73	57.33	55.65	0.04	0.09	44.70	56.89
TiO ₂	0.00	0.00	0.00	0.00	0.00	0.00	0.00	0.10	0.00	0.13	0.03
Al ₂ O ₃	0.00	22.99	4.87	1.05	2.19	0.81	1.82	26.68	65.96	13.85	1.20
Cr ₂ O ₃	0.000	0.48	0.16	0.21	0.00	0.00	0.03	37.29	0.85	1.23	0.21
FeO	12.239	10.94	3.36	1.66	8.05	7.55	9.71	22.97	11.71	3.77	2.25
MnO	0.210	0.45	0.09	0.02	0.08	0.18	0.14	0.34	0.15	0.04	0.05
MgO	47.510	17.64	17.65	17.42	33.69	34.13	32.80	10.28	20.73	18.58	23.33
CaO	0.029	6.16	21.320	24.680	0.130	0.110	0.189	0.00	0.04	12.57	13.27
Na ₂ O	0.000	0.00	0.290	0.500	0.000	0.000	0.093	0.00	0.00	2.36	0.13
K ₂ O	0.000	0.00	0.010	0.010	0.000	0.000	0.027	0.00	0.00	0.07	0.02
Total	100.61	100.39	100.699	100.834	100.865	100.105	100.468	97.70	99.53	97.30	97.38
Si	1.000	2.993	1.901	1.984	1.949	1.982	1.941	0.001	0.002	6.287	7.823
Ti	0.000	0.000	0.000	0.000	0.000	0.000	0.000	0.002	0.000	0.014	0.003
Al	0.000	1.943	0.206	0.044	0.089	0.033	0.075	0.983	1.952	2.296	0.195
Cr	0.000	0.027	0.005	0.006	0.000	0.000	0.001	0.921	0.017	0.137	0.023
Fe ²⁺	0.252	0.653	0.099	0.048	0.231	0.218	0.283	0.591	0.243	0.406	0.258
Mn	0.004	0.027	0.003	0.001	0.002	0.005	0.004	0.009	0.003	0.005	0.005
Mg	1.74	1.886	0.944	0.932	1.725	1.758	1.706	0.479	0.775	3.894	4.783
Ca	0.00	0.474	0.820	0.949	0.005	0.004	0.007	0.000	0.001	1.894	1.956
Na	0.00	0.000	0.020	0.035	0.000	0.000	0.006	0.000	0.000	0.644	0.036
K	0.00	0.000	0.000	0.000	0.000	0.000	0.001	0.000	0.000	0.013	0.004
Total	3.000	8.003	3.998	3.999	4.001	4.000	4.025	2.986	2.993	15.590	15.085
X _{Mg}	0.87	0.75	0.90	0.95	0.89	0.89	0.86	0.45	0.76	0.98	0.95
Cr*								0.48	0.86		

Analyses (in wt%) of olivine (Ol), garnet (Grt), clinopyroxene (Cpx), orthopyroxene (Opx), spinel (Spl) and amphibole (Amp). Olivine is normalized to 4, garnet to 12, clinopyroxene to 6, orthopyroxene to 6, spinel to 4 and amphibole to 23 oxygens. Exs - exsolution in clinopyroxene.

Garnet-olivine Fe^{2+} -Mg exchange geothermometry

Garnet-olivine Fe^{2+} -Mg exchange thermometer is based on the partitioning of iron and magnesium between the coexisting garnet and olivine and may be represented by the exchange reaction:



The distribution coefficient K_D is defined as:

$$K_D = \frac{X_{Mg}^{ol} \cdot X_{Fe}^{grt}}{X_{Fe}^{ol} \cdot X_{Mg}^{grt}}$$

where X_{Mg}^{ol} is the mole fraction of Mg in olivine, X_{Fe}^{grt} is the mole fraction of Fe^{2+} in the garnet, etc.

Garnet-olivine Fe^{2+} -Mg exchange thermometer has been successfully calibrated by O'NEILL & WOOD (1979) and later corrected by O'NEILL (1980) yielding the following equation:

$$\begin{aligned} T_{OW-80} (^{\circ}C) = & \\ = & \frac{902 + DV + (X_{Mg}^{ol} - X_{Fe}^{ol}) \cdot (498 + 1.51(P - 30))}{\ln K_D + 0.357} + \\ & + \frac{-98 \cdot (X_{Mg}^{grt} - X_{Fe}^{grt}) + 1347 \cdot X_{Ca}^{grt}}{\ln K_D + 0.357} - 273 \end{aligned}$$

DV term is incorporating thermal expansion and compressibilities for all four phases and is given by:

$$\begin{aligned} DV = & 462.5 \cdot (1.0191 + (T - 1073)) \cdot (2.87 \cdot 10^{-5}) \cdot (P - 2.63 \cdot 10^{-4} \cdot P^2 - 29.76) + \\ & + 262.4 \cdot (1.0292 + (T - 1073)) \cdot (4.5 \cdot 10^{-5}) \cdot (P - 3.9 \cdot 10^{-4} \cdot P^2 - 29.65) - \\ & - 454 \cdot (1.020 + (T - 1073)) \cdot (2.84 \cdot 10^{-5}) \cdot (P - 2.36 \cdot 10^{-4} \cdot P^2 - 29.79) - \\ & - 278.3 \cdot (1.0234 + (T - 1073)) \cdot (2.3 \cdot 10^{-5}) \cdot (P - 4.5 \cdot 10^{-4} \cdot P^2 - 29.6) \end{aligned}$$

where P is in kbars. The four parts of the DV term are volume expressions for almandine, forsterite, pyrope and fayalite, respectively. Since the DV term involves temperature, upper equation for T_{OW-80} is best solved iteratively by estimating initial value of T ($^{\circ}C$) at pressure P (kbar). Since the DV term is small, this method converges rapidly. At P equal to the experimental pressure of 30 kbar, the DV term is zero.

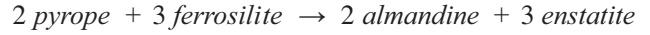
This geothermometer is most sensitive in the temperature and composition regions where K_D is substantially greater than 1. It serves as a reliable geothermometer for magnesium-rich garnet-olivine assemblages equilibrated close to, or within, the temperature range 900–1400 $^{\circ}C$ and pressures up to about 60 kbar. For a fixed K_D , the influence of pressure is to increase the calculated temperature by between 3 and 6 $^{\circ}C$ per kbar (O'NEILL & WOOD, 1979).

In garnet-olivine mineral combination only the garnet is a problematic member because it can incorporate significant amounts of Fe^{3+} in its structure. The presence of a Fe^{3+} component has a considerable influence on the calculated temperatures. The comparison of estimated temperatures for several garnet-olivine pairs with temperatures obtained from two-pyroxene thermometers has shown, that in the case of garnet-olivine thermo-

meter the Fe^{3+} content in garnets can be ignored and all Fe treated as Fe^{2+} (CANIL & O'NEILL, 1996).

Garnet-orthopyroxene Fe^{2+} -Mg exchange geothermometry

The garnet-orthopyroxene Fe^{2+} -Mg exchange thermometer is based on the distribution of Fe^{2+} and Mg between garnet and orthopyroxene according to the reaction:



One of the reliable calibrations of this geothermometer which is applicable to garnet peridotites and granulites was made by HARLEY (1984):

$$T_{H-84} (^{\circ}C) = \frac{3740 + 1400 \cdot X_{Ca}^{grt} + 22.86 \cdot P}{R \cdot \ln K_D + 1.96} - 273$$

where P is pressure in kbars and R is the universal gas constant (8.3143 J/K mol). The distribution coefficient is given by:

$$K_D = \frac{X_{Fe}^{grt} \cdot X_{Mg}^{opx}}{X_{Mg}^{grt} \cdot X_{Fe}^{opx}} = \frac{(Fe^{2+}/Mg)^{grt}}{(Fe^{2+}/Mg)^{opx}}$$

and

$$X_{Ca}^{grt} = \frac{Ca}{Ca + Mn + Fe^{2+} + Mg}$$

The distribution of Fe^{2+} and Mg between garnet and orthopyroxene produces a good geothermometer with required high dP/dT slope and a range in K_D of 4 to 1.5 over geologically attainable P-T conditions. At low temperatures the precision of the geothermometer is limited by analytical uncertainties. An error in K_D of only ± 0.1 is equivalent to ± 40 – 60 $^{\circ}C$ error in temperature estimation (HARLEY, 1984).

The effects of Fe^{3+} calculations are very important when using garnet-orthopyroxene Fe^{2+} -Mg exchange thermometer. Normally, in natural assemblages Fe^{3+} preferentially enters garnet rather than orthopyroxene. K_D values calculated by simply assuming $Fe^{tot} = Fe^{2+}$ will therefore be greater than those calculated by estimating Fe^{3+} with some consistent charge- and mass-balance algorithm. Even a small decrease of K_D , resulting from Fe^{3+} calculation, may raise estimated temperatures by 20–100 $^{\circ}C$, which is a significant amount (HARLEY, 1984). In natural systems, T_{H-84} temperatures calculated with upper equation by ignoring Fe^{3+} should be regarded as minimum temperatures.

Al-in-orthopyroxene geobarometry

Reliable geobarometers suitable for HP/UHP rocks are mostly based on net-transfer reactions involving transfer of Al from tetrahedral to octahedral coordination sites. The Al-in-orthopyroxene barometer has been widely used. The content of Al^{3+} in octahedral sites in orthopyroxene coexisting with garnet is particularly pressure de-

pendent and hence serves as an adequate indicator of the pressure conditions at which the rock has been equilibrated. Several calibrations of this barometer have been performed, as summarized by KROGH RAVNA & PAQUIN (2003). To date, the BREY & KÖHLER (1990) calibration seems to be the most reliable for pressure calculations over a wide pressure range. Pressure is calculated according to the equation:

$$P(\text{kbar}) = \frac{-C_2 - \sqrt{C_2^2 + \frac{4 \cdot C_3 \cdot C_1}{1000}}}{2 \cdot C_3}$$

with

$$\begin{aligned} C_1 &= -R \cdot T \cdot \ln K_D - 5510 + 88.91 \cdot T - 19 \cdot T^{1.2} + \\ &+ 3 \cdot (X_{Ca}^{grt})^2 \cdot 82458 + X_{Mg}^{M1} \cdot X_{Fe}^{M1} \cdot (80942 - 46.7 \cdot T) - \\ &- 3 \cdot X_{Fe}^{grt} \cdot X_{Ca}^{grt} \cdot 17793 - X_{Ca}^{grt} \cdot X_{Cr}^{grt} \cdot (1.164 \cdot 10^6 - \\ &- 420.4 \cdot T) - X_{Fe}^{grt} \cdot X_{Cr}^{grt} \cdot (-1.25 \cdot 10^6 + 565 \cdot T) \\ C_2 &= -832 - 8.78 \cdot 10^{-5} \cdot (T - 298) + 3 \cdot (X_{Ca}^{grt})^2 \cdot 3305 - \\ &- X_{Ca}^{grt} \cdot X_{Cr}^{grt} \cdot 13.45 + X_{Fe}^{grt} \cdot X_{Cr}^{grt} \cdot 10.5 \\ C_3 &= 16.6 \cdot 10^{-4} \end{aligned}$$

R is the universal gas constant (8.3143 J/K mol) and the distribution coefficient is calculated as:

$$K_D = \frac{(1 - X_{Ca}^{grt})^3 \cdot X_{Al}^{grt}}{X_{MF}^{M1} \cdot (X_{MF}^{M2})^2 \cdot X_{Al,TS}^{M1}}$$

Site occupancies for pyroxenes are taken from NICKEL & GREEN (1985) and CARSWELL & GIBB (1987) and are defined as:

$$\begin{aligned} X_{Al}^{M1} &= \frac{Al + Na - Cr - Fe^{3+} - 2 \cdot Ti}{2} \\ X_{Al,TS}^{M1} &= \frac{Al + Na - Cr - Fe^{3+} - 2 \cdot Ti}{2} \quad (\text{for } Jd < 0) \\ X_{Al,TS}^{M1} &= \frac{Al - Na + Cr + Fe^{3+} + 2 \cdot Ti}{2} \quad (\text{for } Jd > 0) \\ X_{Mg}^{Mi} &= X_{MF}^{Mi} \cdot X_{MF} \quad (i = 1, 2) \\ X_{Fe}^{M1} &= X_{MF}^{M1} \cdot (1 - X_{MF}) \\ X_{MF}^{M1} &= (1 - X_{Al}^{M1} - Cr - Fe^{3+} - Ti) \\ X_{MF}^{M2} &= (1 - Ca - Na - Mn) \\ X_{MF} &= \frac{Mg}{Mg + Fe^{2+}} \end{aligned}$$

Site occupancies for garnet are as follows:

$$\begin{aligned} X_{Ca}^{grt} &= \frac{Ca}{Ca + Mg + Fe^{2+} + Mn} \\ X_{Fe}^{grt} &= \frac{Fe^{2+}}{Ca + Mg + Fe^{2+} + Mn} \\ X_{Mg}^{grt} &= \frac{Mg}{Ca + Mg + Fe^{2+} + Mn} \\ X_{Al}^{grt} &= \frac{Al}{Al + Cr} \end{aligned}$$

$$X_{Cr}^{grt} = \frac{Cr}{Al + Cr}$$

Like in the Fe²⁺-Mg geothermometry, the oxidation state of present iron has significant influence. Fe³⁺ is replacing Al³⁺ in octahedral places in orthopyroxene structure. Consequently, equal amounts of Al³⁺ in tetrahedral sites are required to retain charge balance. This results in a limited amount of Al³⁺ available for the substitution, therefore calculated activity of the MgAl₂SiO₆ component in orthopyroxene is considerably underestimated.

Results

Petrography and mineral chemistry

Several samples of relatively well-preserved garnet peridotites from two known localities were investigated: one locality is outcropping within the SBUC near Visole; the other one is exposed farther west, near Prihovca (Figure 3). In Visole the garnet-bearing peridotites occur as very small lenses within the extensively serpentinized ultrabasites while in Prihovca area garnet peridotite bodies of up to several metres in size are exposed within the rocks of continental crustal origin, mainly micaschists and gneisses. Garnet peridotites exhibit rather massive and relatively homogeneous textures without any distinct compositional layering visible in the outcrop, hand-specimen and thin-section scale. In well preserved garnet peridotites big pinkish-red colored garnet grains are surrounded by a black matrix whereas more serpentinized varieties contain completely white colored garnets.

Garnet peridotites consist of garnet, olivine, orthopyroxene, clinopyroxene and brown spinel, which are to a variable extent replaced by amphibole, green spinel, serpentine, talc and chlorite. They show higher modal amounts of garnet and clinopyroxene relative to olivine, therefore they are mainly classified as pyroxenites (garnet-olivine websterites), some of the samples even as garnet orthopyroxenites. However, because of intensive retrogression of these rocks, the abundance of primary minerals is largely obscured.

Garnet mostly forms big porphyroblastic grains with irregular boundaries (Figure 4a). Only rarely it is found in idiomorphic forms with well developed crystal faces. Garnet is also found as exsolution lamellas from clinopyroxene, in form of irregular, bleb-resembling inclusions in orthopyroxene and in coronas around Cr-spinel. All garnets are pyrope-rich, belonging to almandine-pyrope-grossular series. End member compositions are ranging from 53–68 mol% of pyrope, 18–33 mol% of almandine and spessartine, and 8–20 mol% of grossular and andradite. Garnets in samples from Prihovca contain slightly higher pyrope content (56–68 mol%) than garnets from Visole (54–66 mol%).

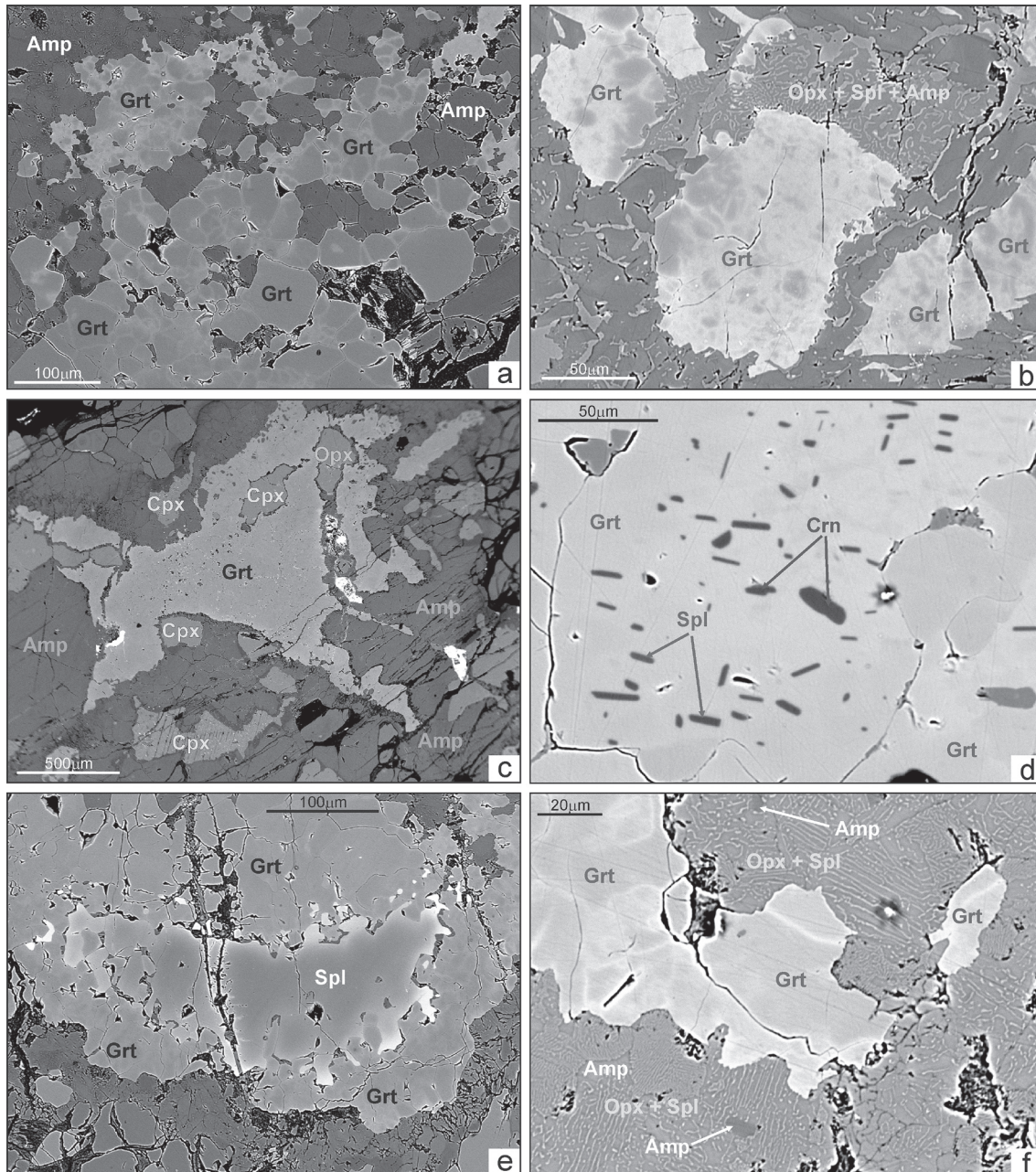


Figure 4. Garnets from garnet peridotites in photomicrographs – backscattered electron images (BSE).

- (a) Inhomogeneous garnet porphyroblasts are mainly found in shape of xenomorphic grains with irregular boundaries.
 (b) Patchy garnet grains surrounded by secondary symplectites of spinel, amphibole and orthopyroxene. Difference between high-Mg dark parts and low-Mg bright parts within same garnet grain is well displayed.
 (c) Big garnet grain with irregular boundaries comprises clinopyroxene and orthopyroxene inclusions. Garnet is surrounded by amphibole and appears homogeneous due to relatively small magnification.
 (d) Corundum and spinel inclusions in inhomogeneous garnet display semi-parallel orientation. Spinel inclusions in this case might be interpreted as remnants of primary low-pressure stage or as secondary minerals. It is also not clear whether corundum minerals are real inclusions or maybe exsolutions from garnet.
 (e) Cr-Spinel inclusion in garnet represents primary spinel overgrown by garnet during subduction.
 (f) Garnet rims are replaced by symplectitic intergrowth of Al-orthopyroxene, Al-spinel, diopside and Prp-amphibole. As a result of retrogression, garnet shows a decrease in Mg (darker parts) and increase in Fe (brighter parts). Amp-amphibole, Cpx-clinopyroxene, Crn-corundum, Grt-garnet, Ol-olivine, Opx-orthopyroxene, Spl-spinel.

The most pronounced feature of garnets from the studied garnet peridotites is their patchy appearance (Figure 4b) caused by chemical inhomogeneity. Patchy garnets were found in samples from both localities, although garnets from Prihovca are slightly more homogeneous than those from Visole. Dark parts of garnets are Mg-rich with 60 to 68 mol% of pyrope and are corresponding to peak pressure compositions. Bright parts are Ca-

and Fe-rich, but Mg-poor with much lower pyrope content (54 to 56 mol%). During decompression, Mg is moving out of garnet which results in enrichment of Ca and Fe. Compositional change between the dark and bright parts in garnets can be well expressed with magnesium number (Mg#):

$$Mg\# = 100 \cdot X_{Mg}^{grt} = 100 \cdot \frac{Mg}{Mg + Fe^{2+}}$$

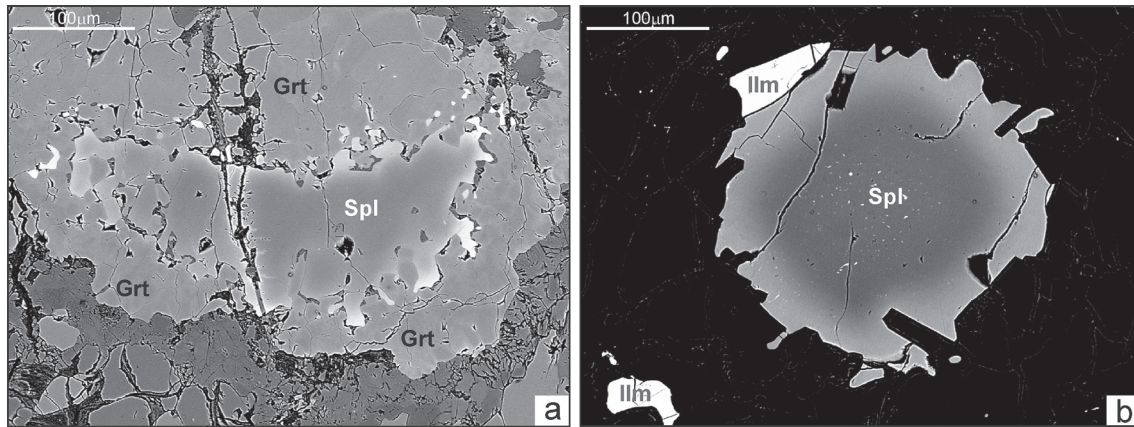


Figure 5. Chromian-rich spinel occurring in matrix (BSE). Matrix minerals in (b) are mostly olivine and amphibole. Both grains show weak zonation indicating an increase of Cr content from core to rim. Amp-amphibole, Cpx-clinopyroxene, Ilm-ilmenite, Ol-olivine, Opx-orthopyroxene, Spl-spinel.

In the dark parts Mg# is reaching 0.78, whereas it never exceeds 0.68 in the bright parts. Relatively slow diffusion processes caused an irregular distribution of composition that resulted in patchy texture of garnet.

Inclusions in garnets are typically clinopyroxene, orthopyroxene (Figure 4c), corundum (Figure 4d) and spinel (Figure 4e). Mg# of garnet close to the interface with clinopyroxene inclusion (0.74) is slightly lower than Mg# of garnet next to orthopyroxene inclusion (0.76) indicating that compositional modification of garnet is higher next to clinopyroxene than next to orthopyroxene. Cr-spinel inclusions are remnants of the primary low-pressure stage that was overgrown by garnet during subduction. Pressure increase and possibly cooling governed formation of garnet on expense of spinel, clinopyroxene and orthopyroxene.

Garnets are replaced by kelyphitic rims consisting of symplectitic intergrowth of high-Al orthopyroxene, Al-rich spinel, diopside and paragasitic amphibole (Figure 4f). Chromium number (Cr*) in Al-spinel is ranging from 0.6–0.9 and is calculated from:

$$Cr^* = 100 \cdot \frac{Cr}{Cr + Al}$$

Kelyphitic assemblage around garnets formed during the exhumation-related decompression of these rocks. Decompressional breakdown of garnet caused the diffusion of Mg and Al in spinel and Ca in clinopyroxene. As a result of retrogression, garnet shows a decrease in Mg and increase in Fe.

Spinel group minerals form two generations, the brown chromian-rich spinel and the green aluminum-rich spinel. Cr-spinel occurs in the matrix (Figure 5a) and as inclusions in garnet (Figure 4d, e). Cr-spinel inclusions are remnants of the primary low-pressure stage that was overgrown by garnet (Figure 4e) during subduction due to pressure increase and possibly cooling.

The composition of Cr-spinel ranges from $Al_2O_3 = 24.3\text{--}53.5$ wt%, $Cr_2O_3 = 13.9\text{--}38.7$ wt% and $Mg\# = 40.7\text{--}68.2$. Cr-spinel shows a weak zoning with

mainly lighter rims and darker cores (Figure 5b). The lighter spinel has a higher chromium number ($Cr^* = 47\text{--}52$) than the darker spinel ($Cr^* = 22\text{--}43$). During the growth, garnet takes up the Al from the spinel, which consecutively becomes more Cr-rich at the rim and thus lighter in color. Al-spinel represents a second generation that may be found in symplectites, mostly with Al-orthopyroxene replacing garnet (Figure 4f). The composition of Al-spinel ranges from $Al_2O_3 = 57.7\text{--}69.6$ wt%, $Cr_2O_3 = 0\text{--}2.8$ wt%, $Mg\# = 76.3\text{--}85.5$ and $Cr^* = 0\text{--}3.1$.

Olivine grains are unzoned and nearly homogeneous in composition (Figure 6a). The chemical homogeneity of olivine may be explained by the fact that olivine is a mineral with fastest diffusion of elements. Fe-Mg diffusion in olivine is about two orders of magnitude faster than in pyroxene and garnet (BRENKER & BREY, 1997). Olivine mainly occurs as matrix mineral sometimes containing clinopyroxene (Figure 6a) and orthopyroxene inclusions. Forsterite content of the studied olivine is ranging in very wide range from 77.0 to 91.0. Olivine contains 0.02–0.28 wt% MnO, <0.07 wt% CaO, <0.02 wt% TiO_2 and <0.15 wt% Cr_2O_3 . NiO content is rather variable and is reaching up to 0.38 wt%.

Olivine is intensively fractured and broken down into smaller grains due to retrogression (Figure 6b). Cracks are filled with secondary opaque minerals. In the contact zones between olivine and garnet extensive kelyphitic coronas have been developed (Figure 6b). They consist of diopsidic clinopyroxene, orthopyroxene, Al-spinel and paragasitic amphibole. Kelyphitisation results from a metamorphic reaction between olivine and garnet during retrogression. The relative abundance of amphibole and clinopyroxene in kelyphitic rims probably reflects local fluctuations of P_{H_2O} during kelyphite growth (GODARD & MARTIN, 2000).

Orthopyroxenes occur as four different types of grains: (1) small inclusions in garnet (Figure 4c); (2) symplectitic intergrowth with Al-spinel replacing garnet (Figure 4f); (3) oriented lamellar exsolutions from clinopyroxene; and (2) individu-

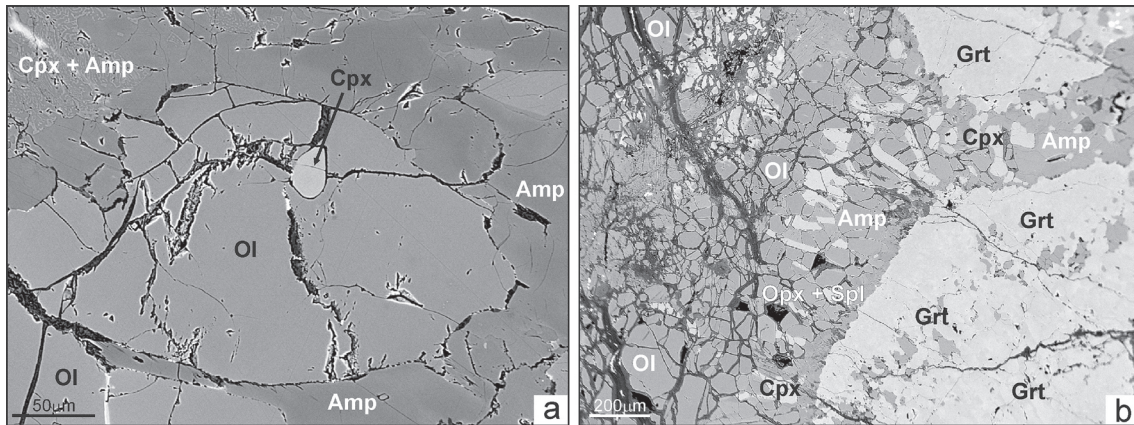


Figure 6. Olivine grains in BSE.

(a) Homogeneous olivine with small clinopyroxene inclusion.

(b) Kelyphitic corona in contact between garnet and olivine. Olivine grains are broken down into numerous individual particles due to retrogression and weathering. Cracks are often filled with opaque secondary minerals. Amp-amphibole, Cpx-clinopyroxene, Grt-garnet, Ol-olivine, Opx-orthopyroxene, Spl-spinel.

al matrix grains (Figure 7). Regardless of their occurrence, grain size and textural origin, the analyzed orthopyroxene grains are very similar in composition. All orthopyroxenes are enstatites ($En = 83.7\text{--}92.1$) with Mg-numbers varying from 83.9 to 92.4. Al_2O_3 and Cr_2O_3 concentrations range from 0.73–2.98 wt% and 0–0.20 wt%, respectively. CaO and TiO_2 contents in all measured orthopyroxenes are low with <0.56 wt% for CaO and <0.05 wt% for TiO_2 . MgO (31.67–35.70 wt%) and MnO contents are typical for worldwide orthopyroxene compositions with MnO in some cases extended to slightly higher values (up to 0.26 wt%).

Matrix orthopyroxenes are found in the form of small rounded grains (Figure 7a) or as large anhedral minerals (Figure 7b). The latter commonly reveal intracrystalline exsolution microstructures, consisting of numerous oriented ilmenite and clinopyroxene lamellas, which precipitated from a supersaturated high-T orthopyroxene host (VAN ROERMUND et al., 2002). Exsolution lamellas exhibit parallel orientation and are concentrated in the central parts of the orthopyroxene grains. The rims of orthopyroxenes are free of exsolutions due to re-crystallization. Some of the orthopyroxenes

reveal internally folded exsolution lamellas (Figure 7b), suggesting that exsolution process was either accompanied or postdated by deformation. Some matrix orthopyroxenes also contain small exsolutions of pargasitic amphibole and garnet. Interstitial garnet exsolutions show very distinct bleb-like shapes (Figure 7b) and are mostly present along the orthopyroxene exsolution-free grain boundary. They show similar microstructures to those reported from garnet websterites in Norway (VAN ROERMUND et al., 2002).

Large matrix orthopyroxene grains are often very low in Al_2O_3 content (down to 0.73 wt%), which reflects high-pressure conditions during their formation. Al content in orthopyroxene is a good diagnostic criteria for revealing pressure variations during the metamorphic evolution. In general, Al decrease can be due to increase in pressure or decrease in temperature (cooling). Inversely, increase in Al content is caused by decompression or heating. High-temperature orthopyroxenes are thus characterized by low Al and high Ca contents. In the analyzed orthopyroxenes the distribution of Al shows lowest Al and highest Ca content in the core. This indicates a decrease in

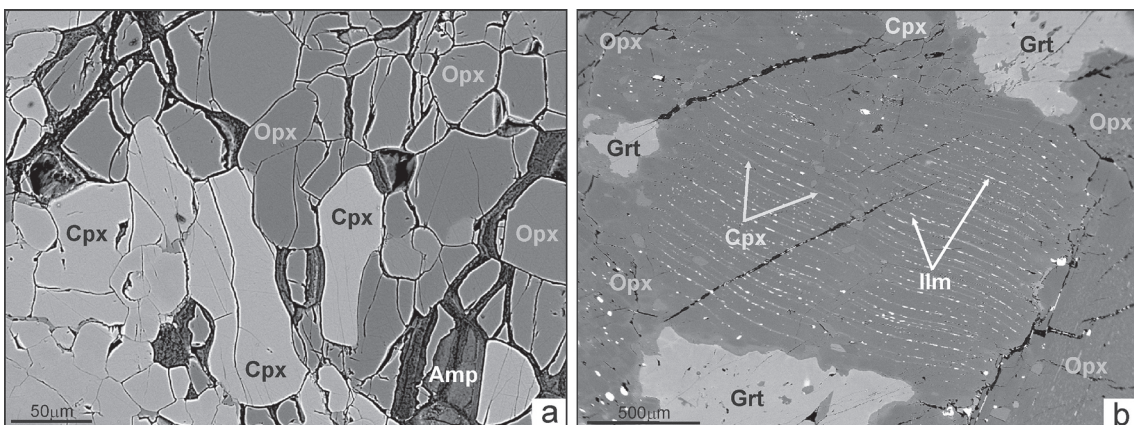


Figure 7. Matrix orthopyroxenes (BSE).

(a) Small rounded orthopyroxene grains in contact with clinopyroxenes and amphiboles.

(b) Banded exsolutions occupying the central part of orthopyroxene grain with re-crystallized, exsolution-free rim. Garnet blebs are arranged along the orthopyroxene grain boundary. Amp-amphibole, Cpx-clinopyroxene, Grt-garnet, Ilm-ilmenite, Opx-orthopyroxene.

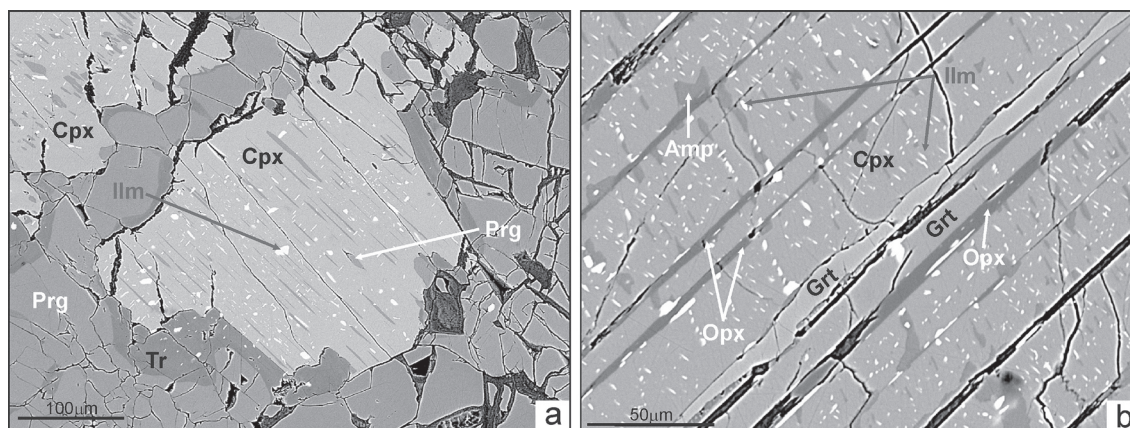


Figure 8. Matrix clinopyroxene grains (BSE).

(a) Individual matrix clinopyroxene grain is rimmed by amphibole and is representing the relict phase of primary material; clinopyroxene inclusions in olivine are also observable.

(b) Garnet, ilmenite and clinopyroxene exsolution within orthopyroxene host exhibit a clearly visible parallel orientation; in some cases the exsolution occur in two perpendicular sets. Amp-amphibole, Cpx-clinopyroxene, Grt-garnet, Ilm-ilmenite, Opx-orthopyroxene, Prg-pargasite, Tr-tremolite.

pressure and temperature from core to rim, consistent with exhumation and decompression of the rocks.

Clinopyroxene occurs in form of matrix grains (Figure 8a), inclusions in garnet (Figure 4c), olivine (Figure 6a) and orthopyroxene, exsolution from orthopyroxene (Figure 7b) and in complex coronas in contact zone between olivine and garnet (Figure 6b). All analyzed clinopyroxenes are diopsides ($En = 46.6\text{--}57.8$, $Fs = 0.1\text{--}6.1$, $Wo = 36.1\text{--}51.0$) with Mg-numbers ranging from 90.0–99.8. They have low Na_2O and Cr_2O_3 content varying from 0.19–0.82 wt% and 0–0.67 wt%, respectively. The Al_2O_3 content is ranging from 0.73–4.87 wt% but TiO_2 content is mostly below 0.13 wt%. No significant compositional differences between clinopyroxene minerals with different occurrence and textural type can be observed. This is taken as good evidence for equilibrium conditions.

Coarse-grained matrix clinopyroxene minerals often contain numerous exsolution lamellas of garnet, low-Al orthopyroxene, ilmenite and pargasitic amphibole (Figure 8b). The size of lamellas is very varied and is ranging from very tiny rods (<10 μm) of ilmenite and orthopyroxene to larger elongated exsolution (up to several 100 μm in length) of garnet and orthopyroxene. Amphibole and some orthopyroxene exsolution are remarkably thicker and relatively short. The obvious intergrowth of different exsolution lamellas and the lack of a clear-cut relationship might suggest a nearly simultaneous generation (XU et al., 2004). All garnet exsolution lie in a direction parallel to the c axis. Some ilmenite lamellas occur in two orientations with nearly perpendicular intersections (Figure 8b), suggesting a topotactical intergrowth due to exsolution rather than being a primary intergrowth or epitaxial replacement (ZHANG & LIOU, 2003).

Matrix clinopyroxene grains are in most cases rimmed by amphiboles of pargasitic and tremolitic composition (Figure 8a).

Other minerals present in the analyzed garnet peridotites and pyroxenites were formed after peak pressure conditions and are related to retrogression due to the exhumation of these rocks. These are typically amphibole, chlorite, serpentine and talc. With decreasing temperature, pargasitic amphibole that is replacing clinopyroxene and which might be stable at pressure conditions up to 25 kbar, is successfully transformed to tremolite, chlorite and serpentine minerals.

Amphibole occurs in 3 different generations: (1) pargasite; (2) tremolite; and (3) gedrite. Bright Na-rich amphibole belongs to pargasite compositions with Mg-number ranging from 89.9–98.1. Pargasitic amphiboles occur around matrix clinopyroxene grains in form of retrogressive rims (Figure 8a), as exsolution in clinopyroxene (Figure 8) and in kelyphitic intergrowth replacing the contact zone between garnet and olivine (Figure 6b). A common retrogression product of ultramafic rocks is also orthoamphibole of gedritic composition. It is known to be forming in lower amphibolite facies conditions, possibly by reactions involving chlorite. The amphibolitization process postdated the formation of symplectitic replacement rims around major mineral phases. In some cases amphibole grains resemble inclusions or have idiomorphic forms, but they are always connected to the periphery with fluid channels and are thus indisputably of secondary origin.

Chlorite, serpentine and talc formed under lowest P-T conditions as late retrogressive stages partly replacing olivine and pyroxene minerals.

Geothermobarometry

Metamorphic conditions for the formation of garnet peridotites have been calculated from a combination of the garnet-olivine (O'NEILL & WOOD, 1979; O'NEILL, 1980) and garnet-orthopyroxene (HARLEY, 1984) Fe^{2+} -Mg exchange thermometers, and Al-in-orthopyroxene barometer (BREY & KÖHLER, 1990).

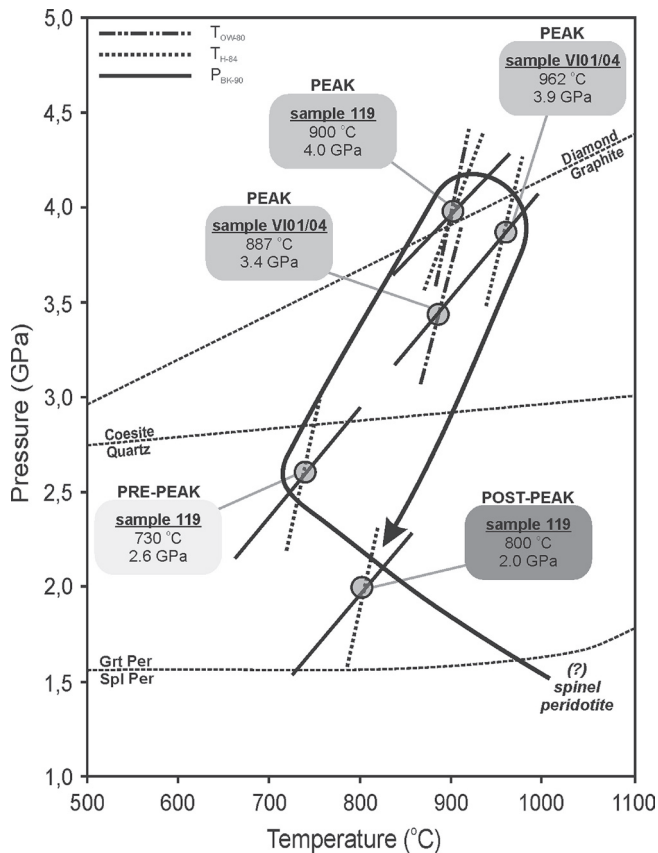


Figure 9. Estimated pressure and temperature conditions with suggested metamorphic P-T path for Pohorje garnet peridotites. A combination of garnet-olivine Fe^{2+} -Mg exchange thermobarometer (OW-80; O'NEILL & WOOD, 1979), garnet-orthopyroxene Fe^{2+} -Mg exchange thermobarometer (H-84; HARLEY, 1984), and Al-in-orthopyroxene barometer (BK-90; BREY & KÖHLER, 1990). Shown for reference are equilibria for diamond-graphite (BUNDY, 1980), coesite-quartz (BOHLEN & BOETTCHER, 1982), and spinel-garnet peridotite (O'HARA et al. 1971).

The initial (pre-peak) metamorphic conditions have been calculated with the application of Fe^{2+} -Mg garnet-orthopyroxene exchange thermometer together with the Al-in orthopyroxene barometer to the garnet and orthopyroxene exsolutions in primary clinopyroxene. Estimated P-T values are 730 °C at pressure of 2.6 GPa.

Porphyroblastic garnet with the highest pyrope content and orthopyroxene with the lowest Al content together with relatively homogeneous olivine have been chosen to calculate peak P-T conditions, as it is generally recommended (e.g. BREY & KÖHLER, 1990; BRENKER & BREY, 1997; KROGH RAVNA & PAQUIN, 2003). The results indicate that the peak of metamorphism occurred at temperatures of 887–962 °C and pressures of 3.4–4.0 GPa (Figure 9). The equilibrium P-T conditions for the sample 119 cluster in a narrow range, close to values of 900 °C and 4 GPa. There is a very good consistency between the garnet-olivine and garnet-orthopyroxene Fe^{2+} -Mg exchange thermometers for this sample. The P-T conditions for sample VI01/04, obtained from the garnet-olivine thermometer and the Al-in-orthopyroxene barometer, are 887 °C and 3.4 GPa, whereas the intersection between the garnet-orthopyroxene thermometer and the Al-in-orthopyroxene barometer yields

962 °C and 3.9 GPa. This discrepancy may result from partial disequilibrium between garnet, olivine and orthopyroxene during post-peak decompression. Additionally, since all Fe has been treated as Fe^{2+} in the calculations, the temperature obtained by garnet-orthopyroxene thermometer should only be regarded as minimum peak temperature (HARLEY, 1984).

The post-peak metamorphic conditions have been deduced from the composition of orthopyroxene in symplectites with Al-rich spinel that form kelyphitic rims around garnet. The garnet-orthopyroxene Fe^{2+} -Mg exchange thermometer in combination with the Al-in-orthopyroxene barometer yields P-T conditions of ~800 °C and 2 GPa.

Discussion and Conclusions

The geothermobarometrical data obtained from garnet peridotites, with peak P-T conditions of 887–962 °C and 3.4–4.0 GPa, clearly confirm the existence of UHP metamorphism in the Pohorje area. Recorded peak metamorphic conditions are in the same range as peak conditions determined for the associated kyanite eclogites (JANÁK et al., 2004; VRABEC, 2010). This confirms that the south-easternmost parts of the Austroalpine nappes in the Alps reached UHP metamorphic conditions during the Cretaceous orogeny at ca. 91–92 Ma. Garnet peridotites were most probably introduced to the subducting plate from the overlying mantle wedge and later on subducted further to the depths of at least 120 km.

From observed mineral assemblages and estimated P-T conditions a metamorphic P-T path can be deduced (Figure 9). The reaction textures, mineral compositions and thermobarometric evidence indicates that garnet-bearing peridotites have undergone a complex history, including at least four stages of recrystallization: protolith stage, metamorphic stage, decompression stage, and retrogression stage.

Stage I: the protolith stage, is garnet-free and is defined by assemblage of olivine + Al-orthopyroxene + Al-clinopyroxene + Cr-spinel. Al-orthopyroxene occurs as inclusions in garnet, whereas Cr-spinel is additionally preserved in the matrix. The initial composition of the investigated peridotite most probably corresponded to spinel lherzolite. The occurrence of Cr-spinel as inclusions in garnet indicates that garnet peridotites evolved from spinel-bearing protolith, which could therefore represent pieces of intermediate to shallow-level lithospheric mantle.

Stage II: the metamorphic stage, is defined by the matrix assemblage of garnet + clinopyroxene + orthopyroxene + olivine + Cr-spinel. Garnet occurs as coronas around Cr-spinel, as exsolutions from clinopyroxene, and as large porphyroblasts in the matrix. Primary, coarse-grained clinopyroxene contains exsolution rods of garnet, low-Al

orthopyroxene, pargasitic amphibole, Cr-spinel and ilmenite.

Formation of garnet exsolutions from clinopyroxene could have started at P-T conditions of about 700–750 °C and 2.5 GPa, as deduced from geothermobarometry. The exsolution process may correspond to the incorporation of peridotite from the overlying mantle wedge into subducting crust. The interaction between the hot mantle and the relatively colder subducting crust probably caused nearly isobaric cooling from spinel to garnet stability field. Similar exsolutions have been observed in other HP and UHP ultramafic rocks, e.g. garnet peridotite and pyroxenite from Nonsberg area, Eastern Alps (GODARD et al., 1996), garnet clinopyroxenite from Sulu, eastern China (ZHANG & LIOU, 2003) and garnet websterite from Bardane, western Norway (CARSWELL & VAN ROERMUND, 2005). The formation of exsolutions in clinopyroxene is undoubtedly caused by reactions driven by changes in temperature and pressure, but the accurate conditions are difficult to estimate. The parent phase of such intergrowths of clinopyroxene + garnet + ilmenite could have been the primary clinopyroxene (ZHANG & LIOU, 2003). Formation of garnet lamellas in clinopyroxene has generally been interpreted as a result of exsolution from primary clinopyroxene (DAWSON & REID, 1970; HARTE & GURNEY, 1975; SAUTTER & HARTE, 1988). According to experimental work of HARTE & GURNEY (1975) a single clinopyroxene is stable in a wedge shaped P-T stability field below the solidus (~3.4–3.8 GPa at 1380–1400 °C; 2.6 GPa at 1370 °C). With decreasing temperature, garnet first appears at ~1400 °C and 3.4–3.6 GPa, joining the clinopyroxene and forming a clinopyroxene + garnet assemblage. Hence, the exsolution of garnet from clinopyroxene has been suggested to be related mainly to cooling from near-solidus conditions toward normal mantle lithosphere temperatures. Although the effect of Ti was not evaluated in HARTE & GURNEY (1975) experiments, a similar clinopyroxene precursor of the garnet + ilmenite + clinopyroxene intergrowth is suggested, as the solubility of clinopyroxene (CaMgSi₂O₆) in garnet is limited except for majorite formed at very high pressures (see Fig. 6 in ZHANG & LIOU, 2003).

During the peak of metamorphism large porphyroblastic garnet was formed from primary, Al-bearing phases such as spinel, clinopyroxene and orthopyroxene. The increased chromium content in the rims implies that Cr-rich spinel (Cr* = c. 50) remained stable at peak metamorphic conditions, since chromium moves the spinel-garnet transition boundary towards higher pressures (WEBB & WOOD, 1986; KLEMME, 2004). P-T conditions of the peak metamorphic stage calculated from geothermobarometry are 887–962 °C and 3.4–4.0 GPa, that is well within the stability field of coesite.

Stage III: the decompression stage, occurred after peak pressure conditions and is manifested by formation of kelyphitic rims of high-Al orthopyroxene, Al-spinel, diopside and pargasitic amphibole replacing garnet. After having reached their

metamorphic peak, the garnet peridotites were exhumed to mid-crustal levels. The composition of orthopyroxene in symplectites with Al-rich spinel was used to obtain P-T conditions during decompression. The garnet-orthopyroxene Fe²⁺-Mg exchange thermometer in combination with the Al-in-orthopyroxene barometer yields P-T conditions of ~800 °C and 2 GPa.

Stage IV: the retrogression stage, occurred under lowest P-T conditions and is characterized by the formation of tremolitic amphibole, gedrite, chlorite, serpentine and talc. Pargasitic amphibole was partly replaced by tremolite, pyroxene by serpentine and chlorite, and olivine by serpentine and talc. It is assumed that pressure and temperature further decreased during this stage. The increased activity of H₂O caused retrogression under low P-T conditions.

References

- BECKER, H. 1993: Garnet peridotite and eclogite Sm-Nd mineral ages from the leontine dome (Swiss Alps): new evidence for Eocene high-pressure metamorphism in the central Alps. *Geology* (New York) 21: 599–602.
- BOHLEN, S.R. & BOETTCHER, A.L. 1982: The quartz-coesite transformation: A precise determination and effects of other components. *J. Geophys. Res.* (Washington) 87: 7073–7078.
- BRENKER, F.E. & BREY, G.P. 1997: Reconstruction of the exhumation path of the Alpe Arami garnet-peridotite body from depths exceeding 160 km. *J. Metamorphic Geol.* (Oxford) 15: 581–592.
- BREY, G.P. & KÖHLER, T. 1990: Geothermobarometry in four-phase lherzolites II. New thermometers, and practical assessment of existing thermobarometers. *J. Petrol.* (Oxford) 31: 1353–1378.
- BRUECKNER, H.K. & MEDARIS, L.G. 2000: A general model for the intrusion and evolution of 'mantle' garnet peridotites in high-pressure and ultra-high-pressure metamorphic terranes. *J. Metamorphic Geol.* (Oxford) 18: 123–133.
- BUNDY, F.R. 1980: The P, T phase and reaction diagram for elemental carbon. *J. Geophys. Res.* (Washington) 85: 6930–6936.
- CANIL, D. & O'NEILL, H. ST. C. 1996: Distribution of ferric iron in some upper mantle assemblages. *J. Petrol.* (Oxford) 37: 609–635.
- CARSWELL, D.A. & GIBB, F.G.F. 1987: Evaluation of mineral thermometers and barometers applicable to garnet lherzolite assemblages. *Contrib. Mineral. Petrol.* (Berlin) 95: 499–511.
- CARSWELL, D.A. & COMPAGNONI, R. 2003: Introduction with review of the definition, distribution and geotectonic significance of ultrahigh-pressure metamorphism. In: CARSWELL, D.A. & COMPAGNONI, R. (eds.): *Ultra-high pressure metamorphism*. EMU Notes in Mineralogy, 5. Eötvös University Press (Budapest): 1–508 cd-rom.
- CARSWELL, D.A. & VAN ROERMUND, H.L.M. 2005: On multi-phase mineral inclusions associated with microdiamond formation in mantle-derived

- peridotite lens at Bardane on Fjortoft, west Norway. *Eur. J. Mineral. (Stuttgart)* 17: 31–42.
- CHOPIN, C. 2003: Ultrahigh-pressure metamorphism: tracing continental crust into the mantle. *Earth Planet. Sci. Lett. (Amsterdam)* 212: 1–14.
- DAWSON, J.B. & REID, A.M. 1970: A pyroxene-ilmenite intergrowth from the Monastery Mine, South Africa. *Contrib. Mineral. Petrol. (Berlin)* 26: 296–301.
- DOBZHINETSAYA, L.F., GREEN, H.W. & WANG, S. 1996: Alpe Arami: a Peridotite Massif from depths of more than 300 km. *Science (Washington)* 271: 1841–1845.
- ERNST, W.G. 1978: Petrochemical study of lherzolitic rocks from the Western Alps. *J. Petrol. (Oxford)* 19: 341–392.
- FODOR, L., JELEN, B., MÁRTON, E., ZUPANČIČ, N., TRAJANOVA, M., RIFELJ, H., PÉCSKAY, Z., BALOGH, K., KOROKNAI, B., DUNKL, I., HORVÁTH, P., VRABEC, M., KRALJIČ, M. & KEVRIČ, R. 2002: Connection of Neogene basin formation, magmatism and cooling of metamorphics in NE Slovenia. *Geol. Carpathica (Bratislava)* 53: 3 cd-rom.
- FODOR, L., BALOGH, K., DUNKL, I., PÉCSKAY, Z., KOROKNAI, B., TRAJANOVA, M., VRABEC, M., VRABEC, M., HORVÁTH, P., JANÁK, M., LUPTÁK, B., FRISCH, W., JELEN, B. & RIFELJ, H. 2003: Structural evolution and exhumation of the Pohorje-Kozjak Mts., Slovenia. *Annales Universitatis Scientiarum Budapestinensis, Sectio Geologica (Budapest)* 35: 118–119.
- FODOR, L., GERDES, A., DUNKL, I., KOROKNAI, B., PÉCSKAY, Z., TRAJANOVA, M., BALOGH, K., HORVÁTH, P., JELEN, B., VRABEC, M. & VRABEC, M. 2007: Formation age, exhumation and deformation of the Pohorje pluton: implications for Cretaceous and Miocene deformations of the Eastern Alps - Pannonian basin junction. Abstract volume, 8th Workshop on Alpine Geological Studies, Davos, 10.-12. October 2007, (Davos): 18–19.
- GEBAUER, D. 1996: A P-T-t path for an (ultra?) high pressure ultramafic/mafic rock-association and its felsic country-rocks based on SHRIMP-dating of magmatic and metamorphic zircon domains. Example: Alpe Arami (Central Swiss Alps). In Basau, A. & Hart, S. (eds.): *Earth Processes. Reading the Isotopic Code*. American Geophysical Union (Washington), Geophysical Monograph 95: 307–329.
- GODARD, G. & MARTIN, S. 2000: Petrogenesis of kelyphites in garnet peridotites: a case study from the Ulten zone, Italian Alps. *J. Geodynamics (New York)* 30: 117–145.
- GODARD, G., MARTIN, S., PROSSER, G., KIENAST, J.R. & MORTEN, L. 1996: Variscan migmatites, eclogites and garnet-peridotites of the Ulten zone, Eastern Austroalpine system. *Tectonophysics (New York)* 259: 313–341.
- HARLEY, S.L. 1984: An experimental study of the partitioning of Fe and Mg between garnet and orthopyroxene. *Contrib. Mineral. Petrol. (Berlin)* 86: 359–373.
- HARTE, B. & GURNEY, J.J. 1975: Evolution of clinopyroxene and garnet in an eclogite nodule from the Roberts Victor kimberlite pipe, South Africa. *Physics and Chemistry of the Earth (New York)* 9: 367–387.
- HINTERLECHNER-RAVNIK, A. 1987: Granatov peridotit na Pohorju. *Geologija (Ljubljana)* 30: 149–181.
- HINTERLECHNER-RAVNIK, A., SASSI, F.P. & VISONA, D. 1991: The Austridic eclogites, metabasites and metaultrabasites from the Pohorje area (Eastern Alps, Yugoslavia): 2. 2. The metabasites and metaultrabasites, and concluding considerations. *Rendiconti Fische Accademia Lincei (Milano)* 2: 175–190.
- HOINKES, G., KOLLER, F., RANTITSCH, G., DACHS, E., HÖCK, V., NEUBAUER, F. & SCHUSTER, R. 1999: Alpine metamorphism of the Eastern Alps. *Schweiz. Mineral. Petrogr. Mitt. (Zürich)* 79: 155–181.
- JANÁK, M., FROITZHEIM, N., LUPTÁK, B., VRABEC, M. & KROGH RAVNA, E.J. 2004: First evidence for ultrahigh-pressure metamorphism of eclogites in Pohorje, Slovenia: Tracing deep continental subduction in the Eastern Alps. *Tectonics, (Washington)* 23: TC5014, doi:10.1029/2004TC001641.
- JANÁK, M., FROITZHEIM, N., VRABEC, M., KROGH RAVNA, E.J. & DE HOOG, J.C.M. 2006: Ultrahigh-pressure metamorphism and exhumation of garnet peridotite in Pohorje, Eastern Alps. *J. Metamorphic Geol. (Oxford)* 24/1: 19–31.
- JANÁK, M., CORNELL, D., FROITZHEIM, N., DE HOOG, J.C.M., BROSKA, I., VRABEC, M., HURAI, V. 2009: Eclogite-hosting metapelites from the Pohorje Mountains (Eastern Alps): P-T evolution, zircon geochronology and tectonic implications. *Eur. J. Mineral. (Stuttgart)* 21/6: 1191–1212.
- KLEMME, S. 2004: The influence of Cr on the garnet-spinel transition in the Earth's mantle: experiments in the system MgO-Cr₂O₃-SiO₂ and thermodynamic modelling. *Lithos (Amsterdam)* 77: 639–646.
- KROGH RAVNA, E.J. & PAQUIN, J. 2003: Thermobarometric methodologies applicable to eclogites and garnet ultrabasites. In: CARSWELL, D.A. & COMPAGNONI, R. (eds.): *Ultra-high pressure metamorphism*. EMU Notes in Mineralogy, 5. Eötvös University Press (Budapest): 1–508 cd-rom.
- LIU, J.G., HANG, W.G.E., RUMBLE, D. & MARUYAMA, S. 1998: High-pressure minerals from deeply subducted metamorphic rocks. In: HEMLEY, R.J. (ed.): *Ultrahigh pressure mineralogy: Physics and chemistry of the Earth's deep interior*. Reviews in Mineralogy, 37. Mineral. Soc. Am.: (Washington): 33–96.
- MEDARIS, L.G. 2000: Garnet peridotites in Eurasian high-pressure and ultrahigh-pressure terranes: A diversity of origins and thermal histories. In: ERNST, W.G. & LIU, J.G. (eds.): *Ultrahigh-pressure metamorphism and geodynamics in collision-type orogenic belts*. International Book Series 4. Geol. Soc. Am. (New York): 57–73.

- MILLER, C. & THÖNI, M. 1997: Eo-Alpine eclogitisation of Permian MORB-type gabbros in the Koralpe (Eastern Alps, Austria): new geochronological, geochemical and petrological data. *Chem. Geol. (New York)* 137: 283–310.
- MILLER, C., MUNDIL, R., THÖNI, M. & KONZETT, J. 2005: Refining the timing of eclogite metamorphism: a geochemical, petrological, Sm-Nd and U-Pb case study from the Pohorje Mountains, Slovenia (Eastern Alps). *Contrib. Mineral. Petrol. (Berlin)* 150: 70–84.
- MIOČ, P. & ŽNIDARČIČ, M. 1977: Osnovna geološka karta SFRJ, list Slovenj Gradec, 1 : 100.000. Zvezni geološki zavod (Beograd).
- NEUBAUER, F. & HÖCK, V. 2000: Aspects of geology in Austria and adjoining areas: introduction. *Mitt. Öster. Min. Ges. (Vienna)* 92: 7–14.
- NICKEL, K.G. & GREEN D.H. 1985: Empirical geothermobarometry for garnet peridotites and applications for the nature of the lithosphere, kimberlites and diamonds. *Earth Planet. Sci. Lett. (Amsterdam)* 73: 158–170.
- NIMIS, P. & MORTEN, L. 2000: P-T evolution of 'crustal' garnet peridotites and included pyroxenites from Nonsberg area (upper Austroalpine), NE Italy: from the wedge to the slab. *J. Geodynamics (New York)* 30: 93–115.
- NIMIS, P. & TROMMSDORFF, V. 2001: Revised thermobarometry of Alpe Arami and other garnet peridotites from the Central Alps. *J. Petrol. (Oxford)* 42: 103–115.
- OBATA, M. & MORTEN, L. 1987: Transformation of spinel lherzolite to garnet lherzolite in ultramafic lenses of the austridic crystalline complex, Northern Italy. *J. Petrol. (Oxford)* 28: 599–623.
- O'HARA, M.J., RICHARDSON, S.W. & WILSON, G. 1971: Garnet-peridotite stability and occurrence in crust and mantle. *Contrib. Mineral. Petrol. (Berlin)* 32: 48–68.
- O'NEILL, H.ST.C. 1980: An experimental study of Fe-Mg partitioning between garnet and olivine and its calibration as a geothermometer: corrections. *Contrib. Mineral. Petrol. (Berlin)* 72: 337.
- O'NEILL, H.ST.C. & WOOD, B.J. 1979: An experimental study of Fe-Mg partitioning between garnet and olivine and its calibration as a geothermometer. *Contrib. Mineral. Petrol. (Berlin)* 70: 59–70.
- PAQUIN, J. & ALTHERR, R. 2001: New constraints on the P-T evolution of the Alpe Arami garnet peridotite body (Central Alps, Switzerland). *J. Petrol. (Oxford)* 42: 1119–1140.
- SAUTTER, V. & HARTE, B. 1988: Diffusion gradients in an eclogite xenolith from the Roberts Victor kimberlite pipe: 1. Mechanism and evolution of garnet exsolution in Al₂O₃-rich clinopyroxene. *J. Petrol. (Oxford)* 29: 1325–1352.
- SCHMID, S.M., FÜGENSCHUH, E., KISSLING, E. & SCHUSTER, R. 2004: Tectonic map and overall architecture of the Alpine orogen. *Eclog. Geol. Helv. (BAsel)* 97: 93–117.
- SCHUSTER, R., KOLLER, F., HOECKE, V., HOINKES, G. & BOUSQUET, R. 2004: Metamorphic structure of the Alps: Eastern Alps. In: OBERHÄNSLI, R. (ed.): Explanatory notes to the Map of Metamorphic Structures of the Alps. *Mitt. Öster. Min. Ges. (Vienna)* 149: 175–199.
- TAKAHASHI, E. 1986: Melting of a dry peridotite KLB-1 up to 14 GPa: Implications on the origin of peridotitic upper mantle. *J. Geophys. Res. (Washington)* 91: 9367–9382.
- THÖNI, M. 2002: Sm-Nd isotope systematics in garnet from different lithologies (Eastern Alps): age results, and an evaluation of potential problems for garnet Sm-Nd chronometry. *Chem. Geol. (New York)* 185: 255–281.
- THÖNI, M. & JAGOUTZ, E. 1992: Some new aspects of dating eclogites in orogenic belts: Sm-Nd, Rb-Sr, and Pb-Pb isotopic results from the Austroalpine Saualpe and Koralpe type locality (Carinthia/Styria, southeastern Austria). *Geochim. Cosmochim. Acta (New York)* 56: 347–368.
- THÖNI, M. & MILLER, C. 1996: Garnet Sm-Nd data from the Saualpe and the Koralpe (Eastern Alps, Austria): chronological and P-T constraints on the thermal and tectonic history. *J. Metamorphic Geol. (Oxford)* 14: 453–466.
- TRAJANOVA, M., PEČSKAY, Z., ITAYA, T. 2008: K-Ar geochronology and petrography of the Miocene Pohorje Mountains batholith (Slovenia). *Geol. Carpath. (Bratislava)* 59: 247–260.
- TUMIATI, S., THÖNI, M., NIMIS, P., MARTIN, S. & MAIR, V. 2003: Mantle-crust interactions during Variscan subduction in the Eastern Alps (Nonsberg-Ulten zone): geochronology and new petrological constraints. *Earth Planet. Sci. Lett. (Amsterdam)* 210: 509–526.
- VAN ROERMUND, H.L.M. & DRURY, M.R. 1998: Ultrahigh pressure (P>6 GPa) garnet peridotites in Western Norway: exhumation of mantle rocks from >185 km depth. *Terra Nova (Oxford)* 10: 295–301.
- VAN ROERMUND, H.L.M., CARSWELL, D.A., DRURY, M.R. & HELBOER, T.C. 2002: Micro-diamonds in a megacrystic garnet-websterite pod from Bardane on the island of Fjortoft, western Norway. *Geology (New York)* 30: 959–962.
- VISONA, D., HINTERLECHNER-RAVNIK, A. & SASSI, F.P. 1991: Geochemistry and crustal P-T polymetamorphic path of the mantle-derived rocks from the Pohorje area (Austrides, Eastern Alps, Slovenia). *Mineralia Slovaca (Bratislava)* 23: 515–525.
- VRABEC, M. 2010: Pohorje eclogites revisited: Evidence for ultrahigh-pressure metamorphic conditions. *Geologija (Ljubljana)* 53/1: see this issue.
- WEBB, S.A. & WOOD, B.J. 1986: Spinel-pyroxene-garnet relationships and their dependence on Cr/Al ratio. *Contrib. Mineral. Petrol. (Berlin)* 92: 471–480.
- XU, W., LIU, X., WANG, Q., LIN, J. & WANG, D. 2004: Garnet exsolution in garnet clinopyroxenite and clinopyroxenite xenoliths in early Cretaceous intrusions from the Xuzhou region, eastern China. *Mineralogical Magazine (London)* 68/3: 443–453.

- ZHANG, R.Y., LIOU, J.G. & CONG B. 1994: Petrogenesis of garnet-bearing ultramafic rocks and associated eclogites in the Su-Lu ultrahigh-P metamorphic terrane, eastern China. *J. Metamorphic Geol. (Oxford)* 12: 169–186.
- ZHANG, R.Y. & LIOU, J.G. 2003: Clinopyroxenite from the Sulu ultrahigh-pressure terrane, eastern China: Origin and evolution of garnet exsolution in clinopyroxene. *Am. Mineral. (Washington)* 88: 1592–1600.
- ZUPANČIČ, N. 1994. Petrografske značilnosti in klasifikacija pohorskih magmatskih kamnin. *Rudarsko metalurški zbornik (Ljubljana)* 41: 101–112.